Hindawi
Advances in Civil Engineering
Volume 2019, Article ID 5943913, 13 pages
https://doi.org/10.1155/2019/5943913

Research Article

Stochastic Inversion Method for Concrete Dams on the Basis of Bayesian Back Analysis Theory

Chongshi Gu,[1,2,3] **Xin Cao**,[1,2,3] **and Bo Xu**[4]

[1]*State Key Laboratory of Hydrology-Water Resources and Hydraulic Engineering, Hohai University, Nanjing 210098, China*
[2]*College of Water Conservancy and Hydropower Engineering, Hohai University, Nanjing 210098, China*
[3]*National Engineering Research Center of Water Resources Efficient Utilization and Engineering Safety, Hohai University, Nanjing 210098, China*
[4]*School of Hydraulic, Energy and Power Engineering, Yangzhou University, Yangzhou 225127, China*

Correspondence should be addressed to Xin Cao; cx_hhu@outlook.com

Received 11 March 2019; Revised 15 August 2019; Accepted 20 August 2019; Published 25 September 2019

Academic Editor: Robert Černý

Inverse analysis is necessary for concrete dams in normal operation to overcome the discrepancy between the true mechanical parameters and test results. In view of the uncertain characteristics of concrete dams, a stochastic inverse model is proposed in this study to solve the undetermined mechanical parameters with sequential and spatial randomness using measured displacement data and Bayesian back analysis theory. An inversion method for the mechanical parameters of concrete dams is proposed. Fast Fourier transform algorithm is introduced to generate random fields for SFEM analysis. The case study shows that the proposed inversion method can reflect the random characteristics of concrete dams, the mechanical parameters obtained are reasonable, and the inverse model is feasible.

1. Introduction

The determination of mechanical parameters is a key issue that affects the accuracy and reliability of positive analysis in the safety assessment of large-scale structures, such as concrete dams [1]. Mechanical parameters are usually obtained from laboratory or in situ tests. However, the results of laboratory tests are influenced by sample disturbance, and in situ tests cannot be conducted extensively due to workload limitations [2]. Thus, the parameters obtained from these tests present large discrepancies with the true values and cannot reflect the real operational situation of projects, especially aging concrete dams [3, 4]. Therefore, the mechanical parameters of concrete dams should be determined through inverse analysis based on prototype observation data [5, 6]. Gu and Wu [7] proposed a deterministic model and a mixed model to obtain the mechanical parameters of concrete dams.

Uncertainties exist in the dam body, dam foundation, and reservoir basin because of the complexity of dam foundation and the heterogeneity of concrete. The corresponding main physical and mechanical parameters usually vary with time and space in a random manner [8, 9]. Therefore, a stochastic inversion method is more suitable for obtaining parameters that can reflect these uncertain characteristics. With its strong capability for nonlinear dynamic processing and mapping highly nonlinear systems, an artificial neural network (ANN) gives more accurate identification results than the conventional methods based on linear models. Aiming at improving the computational efficiency and accuracy of conventional inversion algorithm, the inversion algorithm for random parameters of the dam body, dam foundation, and reservoir basin is put forward using ANN.

In this study, the undetermined physical and mechanical parameters are viewed as random variables with certain probability distributions and spatial variations. Each inversion result is regarded as an implementation of these variables. The objective function is established by utilizing Bayesian back analysis theory. A fast Fourier transform (FFT) algorithm [10] is used to generate Gaussian random

fields for the undetermined parameters. The mean value, variance, and correlation distance of each parameter are obtained using a back-propagation neural network and a stochastic finite element method (SFEM) [11].

A numerical simulation is performed on a certain concrete dam in the commercial finite element software ABAQUS. The mechanical parameters are assigned by utilizing a UMAT subroutine. The inversion algorithm is implemented using the commercial mathematical computing software MATLAB. Results show that the proposed methods can realize stochastic inversion.

2. Basic Principles of the Stochastic Inversion of the Physical and Mechanical Parameters of Concrete Dams

In the stochastic inversion of physical and mechanical parameters, the structural response and the external load are regarded as random variables. The deformation of a concrete dam consists of a hydraulic deformation component, a temperature deformation component, and time-effect deformation component and is defined as [12]

$$\delta = \delta_H + \delta_T + \delta_\vartheta, \tag{1}$$

where δ_H is the hydraulic component, δ_T is the thermal component, and δ_ϑ is the time-effect component.

Hydraulic component δ_H is considered in the inversion of mechanical parameters. After deducing the thermal component and time-effect component, the hydraulic component can be expressed as follows:

$$\boldsymbol{\delta}_H = \mathbf{F}(H, \mathbf{E}), \tag{2}$$

where $\mathbf{F}$ is the export function of the constitutive model, H is the hydraulic load, and $\mathbf{E}$ is an m-dimensional undetermined mechanical parameter vector defined as

$$\mathbf{E} = (E_1, E_2, \ldots, E_m)^{\mathrm{T}}. \tag{3}$$

Undetermined mechanical parameters $E_i\,(i = 1, 2, \ldots, m)$ are regarded as random variables with certain probability distributions represented by the probability distribution function f_i and spatial variations represented by correlation distance θ_i. These parameters are expressed as

$$E_i = g(f_i, \theta_i), \quad i = 1, 2, \ldots, m, \tag{4}$$

where g is the probability distribution function of the undetermined mechanical parameters.

In practical engineering, the set of displacement monitoring points δ_H^* is limited and is a subset of the entire δ_H, $\delta_H^* \in \delta_H$. The displacement function is transformed into

$$\delta_{Hj}^* = F(H, E_i), \quad i = 1, 2, \ldots, m,\ j = 1, 2, \ldots, n, \tag{5}$$

where n is the number of displacement monitoring points.

Structural response variables $\delta_{Hj}^*\,(j = 1, 2, \ldots, n)$ are viewed as random variables in the stochastic inverse analysis. According to Bayesian inversion theory, the error estimation function of back analysis is expressed as [13, 14]

$$\begin{aligned} J(\mathbf{E}) = &\left(\boldsymbol{\delta}_H^* - \boldsymbol{\delta}_H^{\mathrm{cal}}\right)^{\mathrm{T}} \mathrm{cov}^{-1}\left(\boldsymbol{\varepsilon}_{\delta_H^*}\right)\left(\boldsymbol{\delta}_H^* - \boldsymbol{\delta}_H^{\mathrm{cal}}\right) \\ &+ \left(\mathbf{E} - \boldsymbol{\mu}_E\right)^{\mathrm{T}} \mathrm{cov}^{-1}(\mathbf{E})\left(\mathbf{E} - \boldsymbol{\mu}_E\right), \end{aligned} \tag{6}$$

where $\boldsymbol{\delta}_H^*$ is the measured displacement matrix, $\boldsymbol{\delta}_H^{\mathrm{cal}}$ is the corresponding calculated displacement vector, $\mathrm{cov}(\cdot)$ is the covariance matrix, $\boldsymbol{\varepsilon}_{\delta_H^*}$ is the measuring error matrix, $\mathbf{E}$ is the undetermined parameter matrix, and $\boldsymbol{\mu}_E$ is the prior information matrix of $\mathbf{E}$.

Equation (6) is the objective function of Bayesian back analysis. The main objective of stochastic inversion is to obtain the minimum $J(\mathbf{E})$ by generating different matrices $\mathbf{E}$. Variables $\boldsymbol{\delta}_H^*$, $\boldsymbol{\varepsilon}_{\delta_H^*}$, and $\boldsymbol{\mu}_E$ were obtained from monitoring and design information. Therefore, the key to solving the problem is to determine the appropriate method for generating the random variable vector $\mathbf{E}$ and calculate $\boldsymbol{\delta}_H^{\mathrm{cal}}$ through the finite element method.

3. Inverse Analysis Method

Inverse analysis for concrete dams is widely used in determining the elastic modulus of the dam body (E_{c}) and the deformation moduli of the dam foundation (E_{r}) and reservoir basin (E_{b}), which are usually different from the original design values [7]. Therefore, numerical analysis is necessary for the inverse analysis of concrete dams. The current inversion methods are deterministic, and they aim at obtaining the comprehensive mechanical parameters by mean averaging. However, the physical and mechanical parameters of the dam body, foundation, and reservoir basin present randomness and spatial variation characteristics owing to the complexity of geological conditions at the dam site and the heterogeneity of dam body concrete [15]. Numerical simulation involves the simulation of random fields, such as the 3D space random distributions of the mechanical parameters of rock and concrete. Therefore, SFEM is introduced into the stochastic inversion.

3.1. Analysis Model for Stochastic Inversion. The finite element governing equation of the concrete dam system within the linear elastic range is expressed as [16, 17]

$$\mathbf{K}\boldsymbol{\delta} = \mathbf{R}_H, \tag{7}$$

where $\mathbf{K}$ is the overall stiffness matrix, $\boldsymbol{\delta}$ is the node displacement matrix, and $\mathbf{R}_H$ is the node load matrix. $\mathbf{K}$ assumes the following form [7]:

$$\mathbf{K} = \sum_{e_j \in \Omega_1} C_{e_j}^{\mathrm{T}} K_{e_j} C_{e_j} + \sum_{e_j \in \Omega_2} C_{e_j}^{\mathrm{T}} K_{e_j} C_{e_j} + \sum_{e_j \in \Omega_3} C_{e_j}^{\mathrm{T}} K_{e_j} C_{e_j}, \tag{8}$$

where Ω_1, Ω_2, and Ω_3 are the regions of the dam body, dam foundation, and reservoir basin, respectively, and C_{e_j} and K_{e_j} are the stiffness transformation matrix and the stiffness matrix of element e_j, respectively.

In stochastic inversion, the overall stiffness matrix $\mathbf{K}$ in each inversion calculation is regarded as an implementation of the entire stochastic simulation. Monte Carlo simulation is adopted in the stochastic simulation. To

increase calculation efficiency, the Neumann expansion equation is introduced to reduce the calculation times of stiffness matrix inversion.

Stiffness matrix $\mathbf{K}$ is influenced by the fluctuations of the random variables and can be divided into two parts, namely, stiffness matrix $\mathbf{K}_0$ at the mean value of the random variable and fluctuation value $\Delta\mathbf{K}$; thus, $\mathbf{K} = \mathbf{K}_0 + \Delta\mathbf{K}$. According to the Neumann series expansion [18], the inverse matrix $\mathbf{K}^{-1}$ assumes the following form:

$$\begin{aligned}\mathbf{K}^{-1} &= (\mathbf{K}_0 + \Delta\mathbf{K})^{-1} = \left(\mathbf{K}_0\left(\mathbf{I} + \mathbf{K}_0^{-1}\Delta\mathbf{K}\right)\right)^{-1} = \left(\mathbf{I} + \mathbf{K}_0^{-1}\Delta\mathbf{K}\right)^{-1}\mathbf{K}_0^{-1} \\ &= (\mathbf{I} + \mathbf{P})^{-1}\mathbf{K}_0^{-1} = \left(\mathbf{I} - \mathbf{P} + \mathbf{P}^2 + \cdots + (-1)^{m-1}\mathbf{P}^{m-1} + \cdots\right)\mathbf{K}_0^{-1},\end{aligned} \tag{9}$$

where

$$\mathbf{P} = \mathbf{K}_0^{-1}\Delta\mathbf{K}. \tag{10}$$

Equation (7) can be transformed into

$$\boldsymbol{\delta} = \mathbf{K}^{-1}\mathbf{R}_H. \tag{11}$$

If

$$\boldsymbol{\delta}_0 = \mathbf{K}_0^{-1}\mathbf{R}_H, \tag{12}$$

combining equations (9), (11), and (12), the following formula can be obtained:

$$\boldsymbol{\delta} = \boldsymbol{\delta}_0 - \mathbf{P}\boldsymbol{\delta}_0 + \mathbf{P}^2\boldsymbol{\delta}_0 + \cdots + (-1)^{m-1}\mathbf{P}^{m-1}\boldsymbol{\delta}_0. \tag{13}$$

The number of terms in equation (13) is determined according to the accuracy requirement.

If

$$\boldsymbol{\delta}_i = (-1)^{i-1}\mathbf{P}^{i-1}\boldsymbol{\delta}_0, \tag{14}$$

then the following recursive formula can be obtained:

$$\boldsymbol{\delta}_i = -\mathbf{P}\boldsymbol{\delta}_{i-1} = -\mathbf{K}_0^{-1}\Delta\mathbf{K}\boldsymbol{\delta}_{i-1}, \quad (i = 1, 2, 3, \ldots). \tag{15}$$

The Neumann series expansion improves the calculation efficiency of the stochastic simulation by recursion. In the presented method, the stiffness matrix inversion in each Monte Carlo simulation sampling is performed only once. Other simulation samples can be obtained by simply multiplying the fluctuation values [11, 19].

The moments of the displacement responses are obtained by the following equations through the analysis of the concrete dam structure by SFEM:

$$\begin{aligned}E[\delta] &= \frac{1}{N_s}\sum_{i=1}^{N_s}\delta_i, \\ \mathrm{Var}[\delta] &= \frac{1}{N_s}\sum_{i=1}^{N_s}\{\delta_i - E[\delta]\}^2, \\ M_k[\delta] &= \frac{1}{N_s}\sum_{i=1}^{N_s}\{\delta_i - E[\delta]\}^k,\end{aligned} \tag{16}$$

where N_s is the sample number; M_k is the kth-order moment, $k \geq 3$; and $\boldsymbol{\delta}_i$ is the displacement response in the ith stochastic simulation.

3.2. Random Fields of Mechanical Parameters. Three-graded concrete and four-graded concrete are widely used in the construction of concrete dams. However, the dam foundation is a natural rock mass that consists of microcracks, weak layers, and faults. The heterogeneity of concrete and the complexity of dam foundation result in the uncertain characteristics of the mechanical parameters of the dam body, dam foundation, and reservoir basin. Gaussian random fields (GRF) [10, 20] are introduced to describe these mechanical parameters with random characteristics.

The geometric structure and finite elements of the concrete dam calculation model are kept constant during the process of stochastic simulation. Therefore, stiffness matrix [$\mathbf{K}$] in equation (7) is only determined by the random distribution of the mechanical parameters $\mathbf{E}$. Weibull distribution, gamma distribution, and lognormal distribution are common in geotechnical engineering. Thus, the JC method is utilized in this study to transform nonnormal distributions into normal ones. Spatial discretization and spectral decomposition are two common methods for random field generation. An FFT algorithm is introduced to generate the Gaussian random fields of the mechanical parameters of the concrete dam system.

The FFT algorithm is based on the spectral representation of the homogeneous mean-square continuous random fields $Z(x)$, which can be expressed as

$$Z(x) = \int_{-\infty}^{\infty} e^{ix\cdot\omega}W(d\omega), \tag{17}$$

where $W(d\omega)$ is an interval white noise process with zero mean and $S(\omega)d\omega$ variance. $S(\omega)$ is the spectral density function. In practice, the 3D integral for discrete random fields $Z(x_j, x_k, x_p)$ defined on a domain of $K_1 \times K_2 \times K_3$ is expressed as

$$\begin{aligned}Z\left(x_j, x_k, x_p\right) = \lim_{K_1, K_2, K_3 \longrightarrow \infty} \sum_{l=-K_1}^{K_1}\sum_{m=-K_2}^{K_2}\sum_{n=-K_3}^{K_3} A_{lmn}\cos \\ \cdot\left(x_j\omega_l + x_k\omega_m + x_p\omega_n\right) + B_{lmn}\sin \\ \cdot\left(x_j\omega_l + x_k\omega_m + x_p\omega_n\right),\end{aligned} \tag{18}$$

where A_{lmn} and B_{lmn} are Fourier coefficients.

The correlation of a random variable [$X = X(x, y, z)$] in 3D space between points [(x, y, z)] and [$(x + \Delta x, y + \Delta y, z + \Delta z)$] that are defined in the same domain and are, respectively, Δx, Δy, and Δz apart in the three principal axis direction is as follows:

$$\rho[X(x,y,z),X(x+\Delta x,y+\Delta y,z+\Delta z)] = \frac{C[X(x,y,z),X(x+\Delta x,y+\Delta y,z+\Delta z)]}{\sigma_X^2} = \frac{E\{[X(x,y,z)-\mu_X][X(x+\Delta x,y+\Delta y,z+\Delta z)-\mu_X]\}}{\sigma_X^2}, \tag{19}$$

where μ_X is the mean value of X and σ_X^2 is the variance of X.

According to the FFT algorithm, the one-sided spectral density function of a single exponential correlation coefficient is defined as

$$G(\omega_1,\omega_2,\omega_3) = \frac{\sigma^2\theta_1\theta_2\theta_3}{\pi^2\left[1+(\theta_1\omega_1/2)^2\right]\left[1+(\theta_2\omega_2/2)^2\right]\left[1+(\theta_3\omega_3/2)^2\right]}. \tag{20}$$

Use $L = K_1 - l$, $M = K_2 - m$, and $N = K_3 - n$ to denote the symmetric points in fields $K_1 \times K_2 \times K_3$. The variances of the Fourier coefficients in three dimensions are as follows:

$$\begin{aligned} E\left[A_{lmn}^2\right] &= \frac{1}{16}\delta_{lmn}^A\Delta\omega\Big(G_{lmn}^d + G_{lmN}^d + G_{lMn}^d + G_{Lmn}^d \\ &\quad + G_{lMN}^d + G_{LmN}^d + G_{LMn}^d + G_{LMN}^d\Big), \\ E\left[B_{lmn}^2\right] &= \frac{1}{16}\delta_{lmn}^B\Delta\omega\Big(G_{lmn}^d + G_{lmN}^d + G_{lMn}^d + G_{Lmn}^d \\ &\quad + G_{lMN}^d + G_{LmN}^d + G_{LMn}^d + G_{LMN}^d\Big), \end{aligned} \tag{21}$$

where G_{lmn}^d is the spectral density function and d is the number component of $\boldsymbol{\omega} = (\omega_1,\omega_2,\omega_3)$. $\Delta\omega$ and G_{lmn}^d have the form:

$$\begin{aligned} \Delta\omega &= \prod_{i=1}^{3}\Delta\omega_i, \\ G_{lmn}^d &= \frac{G(\omega_l,\omega_m,\omega_n)}{2^d}, \end{aligned} \tag{22}$$

where $\Delta\omega_i$ is an interval of length π/K_i and δ_{lmn}^A and δ_{lmn}^B are given by

$$\begin{aligned} \delta_{lmn}^A &= \begin{cases} 2, & \text{if } l=0 \text{ or } \frac{1}{2}K_1,\ m=0 \text{ or } \frac{1}{2}K_2, n=0 \text{ or } \frac{1}{2}K_3, \\ 1, & \text{otherwise,} \end{cases} \\ \delta_{lmn}^A &= \begin{cases} 0, & \text{if } l=0 \text{ or } \frac{1}{2}K_1,\ m=0 \text{ or } \frac{1}{2}K_2, n=0 \text{ or } \frac{1}{2}K_3, \\ 1, & \text{otherwise.} \end{cases} \end{aligned} \tag{23}$$

4. Inversion Method Based on a BP Neural Network

The inversion of the mechanical parameters of the dam body and foundation can be summarized as an optimization problem. Since the deformation is an implicit equation of mechanical parameters **E**, the back-propagation algorithm of the artificial neural network is introduced into the inversion of the mechanical parameters of the dam body, foundation, and reservoir basin of the concrete dam.

4.1. Basic Theory of BP Neural Network. Artificial neural networks (ANNs) are widely used artificial intelligent algorithms in many fields owing to their excellent capability of modeling nonlinear systems and superior data fitting performance [21]. The feed-forward ANN in Figure 1 consists of an input layer, a hidden layer, and an output layer and can simulate nonlinear mapping from an M-dimensional space to an N-dimensional space [22]. The ANN can perform nonlinear mapping with different precision levels by choosing an appropriate number of nodes in a hidden layer. The back-propagation (BP) algorithm is a mature and widely applied algorithm among ANN algorithms. The hidden layer can be written as

$$b_j = f\left(\sum_{i=1}^{n}\omega_{ij}x_i - \zeta_j\right), \quad (i=1,2,\ldots,n;\ j=1,2,\ldots,s), \tag{24}$$

where b_j is the output of the hidden layer, f is the transfer function, ω_{ij} is the weight from the input layer to the hidden layer, ζ_j is the threshold value of the hidden layer, n is the input node number, and s is the node number of the hidden layer.

The output of the output layer y_k is as follows:

$$y_k = f\left(\sum_{j=1}^{s}\omega_{jk}b_j - \zeta_k'\right), \quad (j=1,2,\ldots,s;\ k=1,2,\ldots,m), \tag{25}$$

where ω_{jk} is the weight from the hidden layer to the output layer, ζ_k' is the threshold value of the output layer, and m is the output node number.

The following sigmoid function is adopted as the transfer function:

$$f(x) = \frac{1}{1+e^{-x}}. \tag{26}$$

The error function of the actual network system output e is as follows:

$$e = \sum_{k=1}^{m}(d_k - y_k)^2, \tag{27}$$

where d_k is the desired output.

The back-propagation algorithm is used in training the ANN. Figure 1 illustrates the architecture of BPNN.

The main steps of BPNN are as follows:

Step 1. Initialize the weights through $\omega_{lq} = \text{Random}(\cdot)$, where lq represents ij or jk.

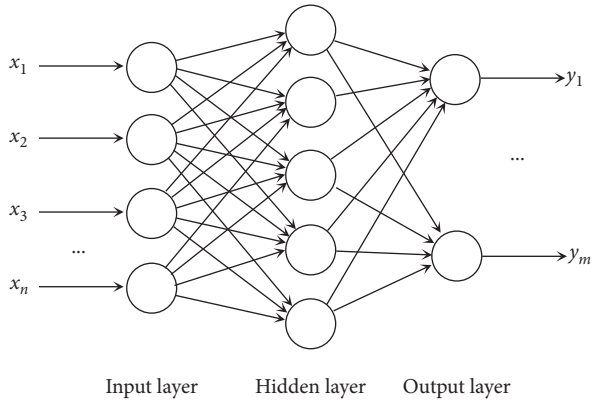

Figure 1: The architecture of back-propagation neural network.

Step 2. Input P learning samples for calculation. Set the current learning sample as the pth sample.

Step 3. Calculate the output b_j and y_k $(j = 1, 2, \ldots, s;\ k = 1, 2, \ldots, m)$ of each layer.

Step 4. Obtain the back-propagation errors of each layer through

$$e_{jk}^{(p)} = \left(d_k^{(p)} - y_k^{(p)}\right) y_k^{(p)} \left(1 - y_k^{(p)}\right), \quad k = 1, 2, \ldots, m, \tag{28}$$

$$e_{ij}^{(p)} = \sum_{k=1}^{m} e_{jk}^{(p)} \omega_{jk} b_j^{(p)} \left(1 - b_j^{(p)}\right), \quad j = 1, 2, \ldots, s. \tag{29}$$

Record the value of $x_i^{(p)}$ and $b_j^{(p)}$.

Step 5. Record the number p of the trained learning sample. If the inequation $p < P$ is satisfied, go to Step 2. If $p = P$, go to Step 6.

Step 6. Revise the weights and thresholds of each layer.

Step 7. Calculate $x_i^{(p)}$ and $b_j^{(p)}$ according to the revised weights. If the inequation $|d_k^{(p)} - y_k^{(p)}| < \varepsilon$ is satisfied for every p and k or the max training time is reached, terminate the training procedure. Otherwise, go to Step 2.

4.2. Deformation Modulus Inversion Method. The inversion of parameters is a process, wherein the basic physical and mechanical parameters are regarded as input variables and the response value δ_{Hj}^{*} $(j = 1, 2, \ldots, n)$ is treated as an approximation under a certain measure, which is the objective function $J(\mathbf{E})$ given by equation (6).

Ranges are assigned the statistical parameters of undetermined mechanical properties as follows:

$$\begin{cases} \mu_{E_i \min} < \mu_{E_i} < \mu_{E_i \max}, & i = 1, 2, \ldots, N, \\ \sigma_{E_i \min} < \sigma_{E_i} < \sigma_{E_i \max}, & i = 1, 2, \ldots, N, \\ \theta_{E_i \min} < \theta_{E_i} < \theta_{E_i \max}, & i = 1, 2, \ldots, N, \end{cases} \tag{30}$$

where $\mu_{E_i \min}$ and $\mu_{E_i \max}$ are the minimum and maximum values of μ_{E_i}, which is the mean value of E_i, respectively; $\sigma_{E_i \min}$ and $\sigma_{E_i \max}$ are the minimum and maximum values of σ_{E_i}, which is the variance of E_i; and $\theta_{E_i \min}$ and $\theta_{E_i \max}$ are the minimum and maximum values of θ_{E_i}, which is the correlation distance of E_i.

The undetermined mechanical parameter E_i can be obtained by searching the minimum $J(\mathbf{E})$ under the end condition given in equation (28). In the inversion algorithm that uses a BP neural network, the statistical parameters are regarded as the nodes in the input layer, and objective function $J(\mathbf{E})$ is considered the output. Subsequently, the map from the former to the latter can be obtained with a small set of training samples. The main steps of the inversion algorithm are as follows:

Step 1. Prior distribution information is obtained, namely, the probability distribution parameters and spatial distribution information of the deformation modulus E_i $(i = 1, 2, \ldots, N)$ on the basis of the design information and laboratory or in situ tests.

Step 2. The nonnormal distributions obtained in Step 1 are transformed into normal ones through the JC method. Prior information $\boldsymbol{\mu}_E$ and correlation $\mathrm{cov}(\mathbf{E})$ of the deformation modulus E_i $(i = 1, 2, \ldots, N)$ are obtained.

Step 3. Deformation modulus E_{0i} $(i = 1, 2, \ldots, N)$ is initialized with the randomly given probability random parameters (i.e., $\mu_{E_{0i}}$, $\sigma_{E_{0i}}$, and $\theta_{E_{0i}}$) and with the constraint $E_{0i} \in [E_{i \min}, E_{i \max}]$.

Step 4. A 3D finite element model for the concrete dam body, dam foundation, and reservoir basin is established.

Step 5. The initial stiffness matrix $\mathbf{K}_0$ is generated according to the established finite element model and the random fields of deformation modulus. Deformation $\boldsymbol{\delta}_0$ is calculated by the finite element method.

Step 6. An implementation of the random fields E_{ki} $(i = 1, 2, \ldots, N;\ k = 0, 1, 2, \ldots)$ is generated by utilizing the FFT algorithm for stochastic simulation based on the given probability random parameters.

Step 7. Fluctuation value $\Delta\mathbf{K}$ and recursive coefficient matrix $\mathbf{P}$ are calculated. The updated deformation is obtained by utilizing the Neumann expansion equation (14).

Step 8: Steps 6–7 are repeated and substituted the calculation results into the error estimation function (6) to obtain $J_k(\mathbf{E})$.

Step 9. Random values are assigned to the probability random parameters $\mu_{E_{ki}}$, $\sigma_{E_{ki}}$, and θ_{E_k}. Steps 5–8 are repeated and a sufficient number of training samples are generated for the BP neural network. The distribution parameters of the mechanical properties can be obtained by minimizing the objective function $J(\mathbf{E})$.

The inversion process is shown with flowchart in Figure 2.

5. Case Study

A concrete gravity dam in southwest China is considered the research object. The crest elevation is 384 m, the minimum

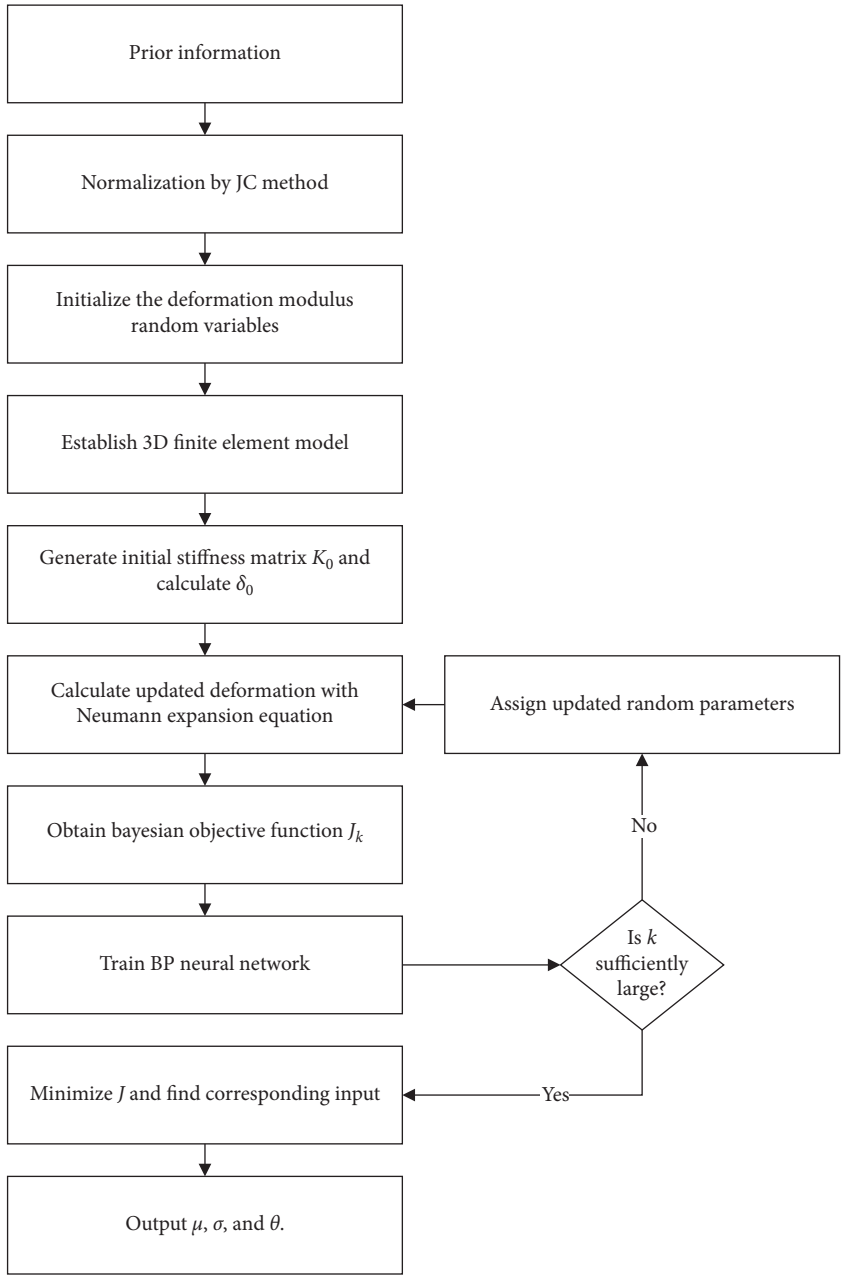

Figure 2: Stochastic inversion algorithm for concrete dams.

foundation surface is 222 m, the maximum dam height is 162 m, and the dam crest length is 909.26 m. The dam body is divided into 43 sections. The normal water level is 380 m, and the dead water level is 370 m. The reservoir storage capacity under normal water level 380 m is 5.16×10^9 m^3, and the effective storage capacity is 9.03×10^8 m^3.

A 3D finite element model of the #7 left-bank water-retaining dam section was established for the back-and-forth analysis of the concrete dam. The model included the dam body, dam foundation, and reservoir basin. The near-dam-area model consisted of the dam body, dam foundation, and reservoir basin. To monitor the dam displacements, a reversed pendulum IP1 was planted at 222 m elevation and three pendulums, namely, PL1-1, PL1-2, and PL1-3, were planted at 322.0, 350.0, and 384.0 m elevations of the dam section, respectively.

The dam section is divided into three zones, namely, A, B, and C, as shown in Figure 3. The concrete of different zones has different concrete grades and strength grades. Table 1 shows the dam body material zoning information of the dam section.

On the basis of the material distributions and the locations of the pendulums, the finite element model was divided into five calculation areas, including the dam body areas A, B, and C, dam foundation, and reservoir basin. The established finite element model was composed of 1590

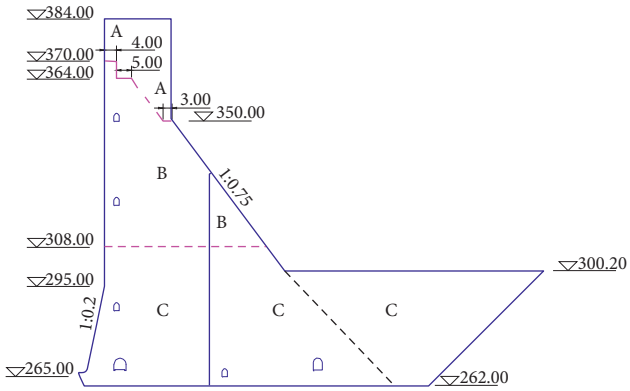

Figure 3: Material zoning of the dam body.

Table 1: The dam body material zoning information.

Zone	Concrete strength grade	Concrete grading
Dam body zone A	$C_{90}25$	Four-graded
Dam body zone B	$C_{180}20$	Three-graded
Dam body zone C	$C_{90}30$	Three-graded

elements and 2392 nodes, among which 333 elements and 536 nodes were for the dam body. Figure 4 shows the finite element mesh.

5.1. Decomposition of the Hydraulic Displacement Component. The time series of the horizontal displacement of the #7 left-bank water-retaining dam section and that of the water level are given in Figure 5 according to the actual pendulum monitoring information. In accordance with dam safety monitoring theory, the statistical models of dam body deformation were established based on the horizontal displacement time series between October 19, 2012, and April 22, 2015, which were monitored by the pendulums and the reversed pendulums. The expression of the established models are as follows:

$$\begin{aligned}\delta = \delta_H + \delta_T + \delta_\vartheta = a_0 + \sum_{i=1}^{3} a_i H^i + \sum_{i=1}^{2} \\ \cdot \left(b_{1i} \sin \frac{2\pi i t}{365} + b_{2i} \cos \frac{2\pi i t}{365}\right) + c_1 \\ \cdot (\vartheta - \vartheta_0) + c_2 (\ln \vartheta - \ln \vartheta_0),\end{aligned} \tag{31}$$

where δ_H, δ_T, and δ_ϑ are, respectively, the hydraulic component, the temperature component, and the time-effect component of the monitored displacement, H is the upstream water head, t is the cumulative days from the initial day to the present day, ϑ_0 is the initial monitoring time which takes 1/100, ϑ is the current monitoring time which takes t/100, and a_0, a_1, a_2, a_3, b_{1i}, b_{1i}, b_{1i}, b_{1i}, c_1, and c_2 are model coefficients.

The hydraulic displacements were obtained by subtracting the temperature component and time-effect component from the horizontal displacements. The measured displacements of different monitoring points are shown in Figure 5. The decomposition results are shown in Figure 6.

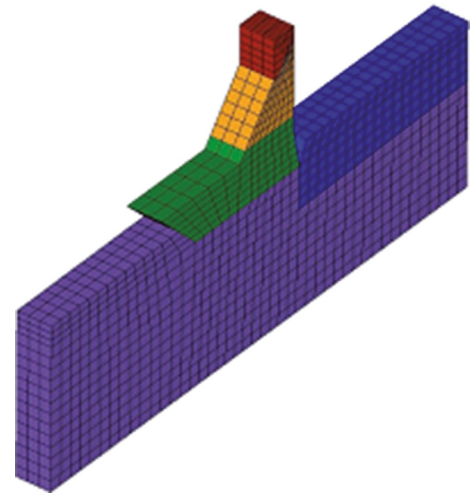

Figure 4: The finite element mesh for the #7 left-bank water-retaining dam section.

5.2. Random Properties of the Undetermined Parameters and Displacement. Mechanical parameter vector **E** consists of five elements, namely, E_{cA}, E_{cB}, E_{cC}, E_r, and E_b. The nonnormal distributions were transformed into normal ones by the JC method. By combining the design information, laboratory material test results, and engineering experience with similar projects, the ranges of the statistical parameters of the mechanical properties were obtained and are given in Table 2.

The input mechanical properties of the finite element model for each stochastic implementation were described by Gaussian random fields, which were generated by the FFT method. Figure 7 exhibits the 2D map of the GRF on the cross section of the dam foundation.

The selected hydraulic structure experienced five impounding processes since the initial impounding in October 2012 and achieved normal water level five times, as shown in Figure 5. The distribution of each measured horizontal displacement was obtained by the stochastic analysis of the measured data at the normal water level. The equivalent normal distribution parameters were obtained by the JC method. The hydraulic displacement components were obtained by subtracting the temperature displacement and the time-effect displacement from the measured data, as shown in Table 3.

5.3. Numerical Simulation with Stochastic FEM. The sample number of each stochastic FEM calculation is 100. The displacement responses and the corresponding modulus distribution are shown in Figure 6 based on the assignment of the random modulus generated in Section 5.2.

Each mechanical parameter E_i was independent of others, and E_i was independent of the displacement errors between the measured data and calculated displacements.

5.4. Inversion Results. Inversion was performed on all five calculation zones of the selected dam section. The zoning deformation modulus is obtained utilizing the initial

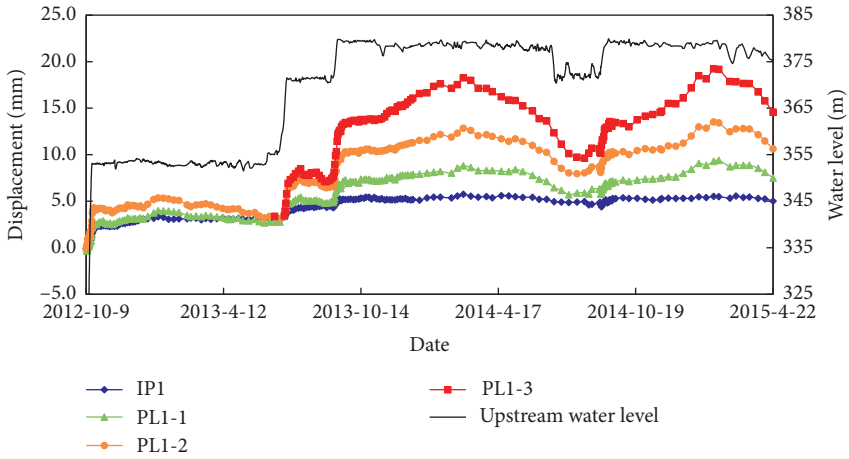

Figure 5: Measured displacements of the #7 left-bank water-retaining dam section.

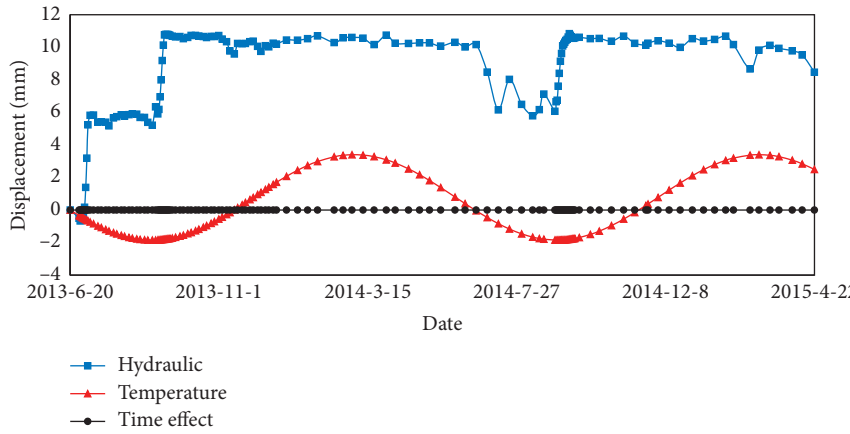

Figure 6: Displacement component result of the monitoring point PL1-1.

Table 2: Initial modulus and ranges of different zones.

Zone	Initial modulus (GPa)	Range of modulus mean value (GPa)		Range of modulus variable coefficient		Range of correlation distance (m)	
		Min	Max	Min	Max	Min	Max
Zone A	27.2	10.0	40.0	0.02	0.3	0.2	10
Zone B	24.1	10.0	40.0	0.02	0.3	0.2	10
Zone C	35.4	10.0	40.0	0.01	0.2	0.2	10
Foundation	26.0	15.0	35.0	0.05	0.3	30	80
Reservoir basin	20.0	10.0	30.0	0.05	0.3	30	80

deformation modulus ranges in Table 2 as optimization constraints and deformation modulus inversion method based on BPNN. The BPNN is trained 1000 times. The inversion results of different calculation zones and comparison with the conventional method are listed in Table 4. The data in Table 4 show that the differences between the inversion results of the stochastic inversion method proposed in this paper and the conventional method are all below 5% which reflect the rationality of the inversion results.

The predicted displacements based on the inversed parameters are listed in Table 5. Figures 8 and 9 show the distribution of the calculated and measured hydraulic displacement of the selected dam body section. Figures 10 and 11 show the comparison between the predicted mean value and variance of hydraulic displacement and the measured data. The comparison of the predicted displacements with the measured data showed that the former are approximate to the latter, verifying the excellence performance of the proposed method.

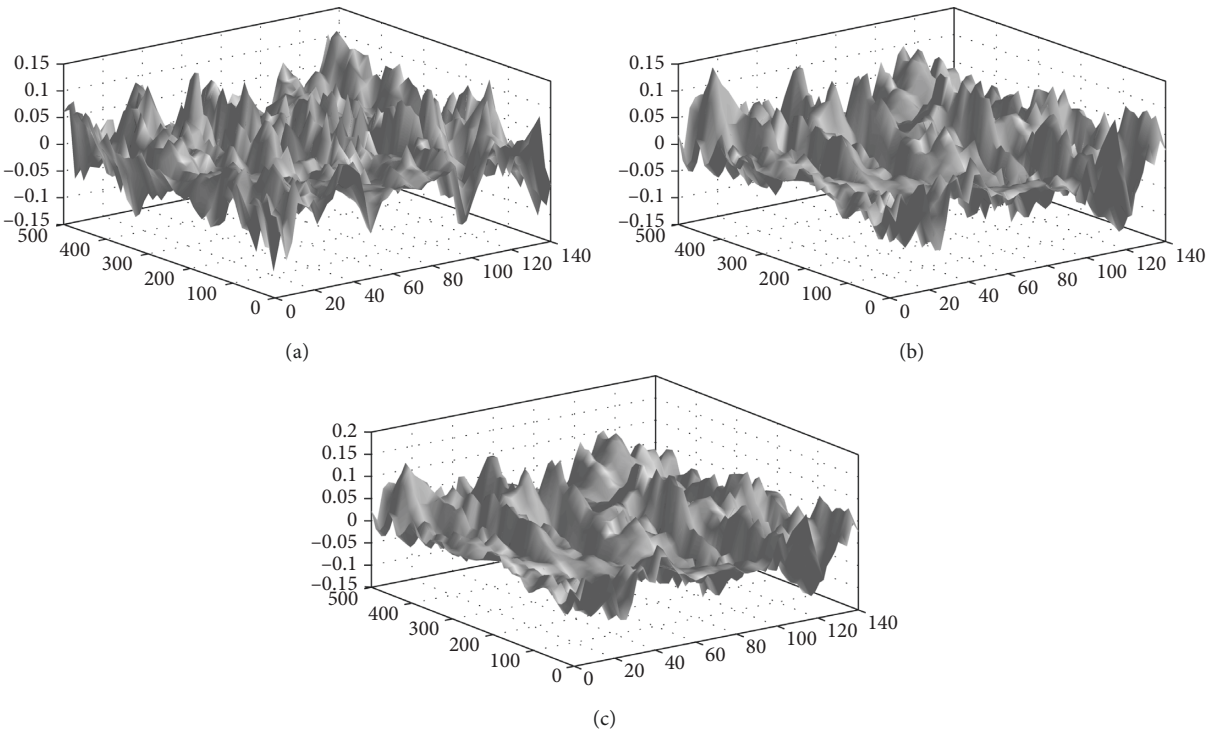

Figure 7: 2D map of the Gaussian random fields: (a) $\theta = 30$ m, (b) $\theta = 50$ m, and (c) $\theta = 80$ m.

Table 3: Properties of the hydraulic displacement component at the normal water level.

Monitoring points	Mean value (mm)	Variance (mm)	Variable coefficient
IP1	3.75	0.052	0.014
PL1-1	5.29	0.098	0.019
PL1-2	7.58	0.15	0.020
PL1-3	10.32	0.19	0.018

Table 4: Inversion results of different calculation zones and comparison with the conventional method.

Calculation zone	Inversed distribution parameters			Inversion results of conventional method
	μ_{E_i} (GPa)	σ_{E_i} (GPa)	θ_{E_i} (m)	E_i (GPa)
Zone A	28.5	0.20	0.51	29.2
Zone B	25.7	0.35	0.73	25.5
Zone C	38.9	2.5	0.75	37.3
Foundation	27.2	3.1	53	28.2
Reservoir basin	23.5	2.4	35	24.1

Table 5: Comparison between the predicted displacement and the measured data.

Monitoring points	$E[\delta_i]$	$\mathrm{Var}[\delta_i]$	$E[\delta_i^{\mathrm{cal}}]$	$\mathrm{Var}[\delta_i^{\mathrm{cal}}]$
IP1	3.75	0.052	3.72	0.072
PL1-1	5.29	0.098	5.36	0.15
PL1-2	7.58	0.15	7.75	0.20
PL1-3	10.32	0.19	10.48	0.27

Figure 12 shows that the true deformation modulus of the dam body, foundation, and reservoir basin is higher than the initial value. This means that the integral stiffness is higher than the design stiffness, which is conducive to the safety of the dam and the foundation. Figures 13 and 14 show the random parameters of deformation modulus of different zones. It can be seen from Figures 13 and 14 that the maximum values of standard

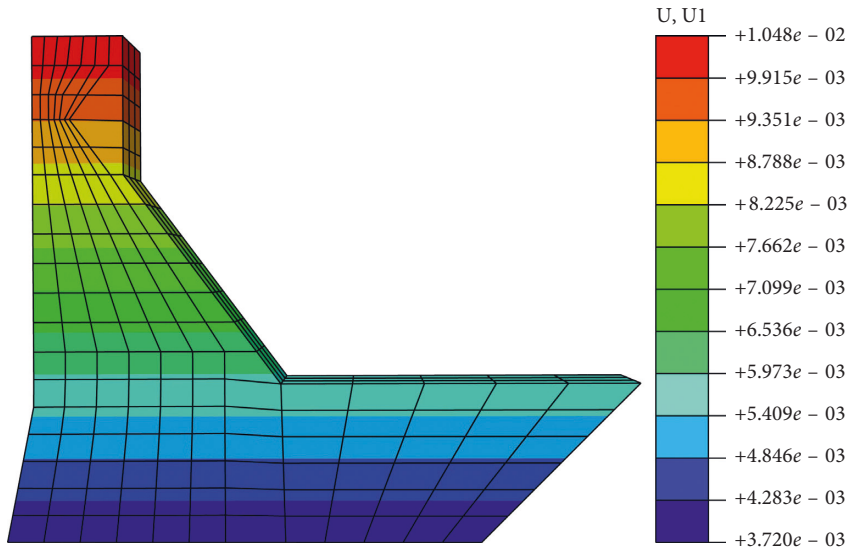

Figure 8: Distribution of the calculated displacement of the selected dam body section.

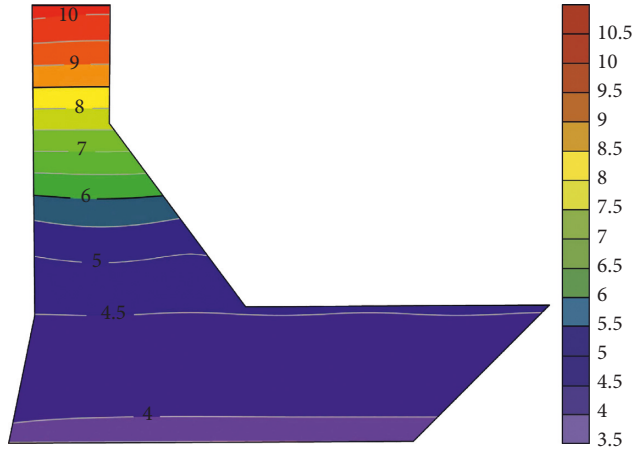

Figure 9: Distribution of the measured hydraulic displacement of the selected dam body section.

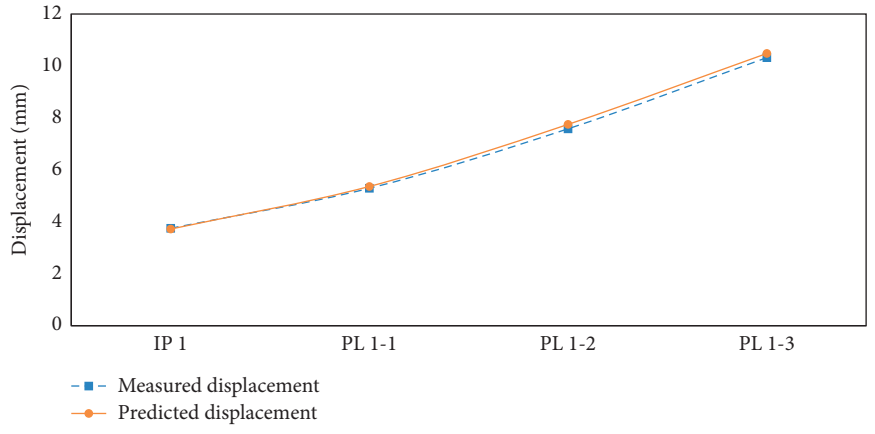

Figure 10: Comparison between the measured displacement and the predicted displacement.

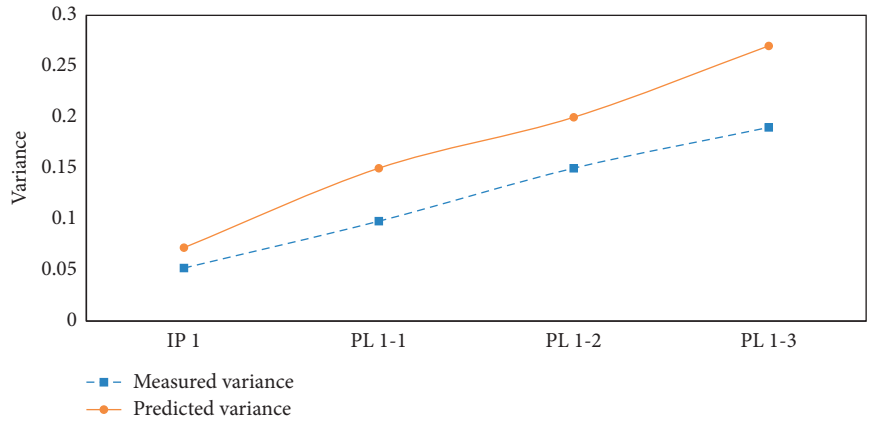

Figure 11: Comparison between the measured variance and the predicted variance.

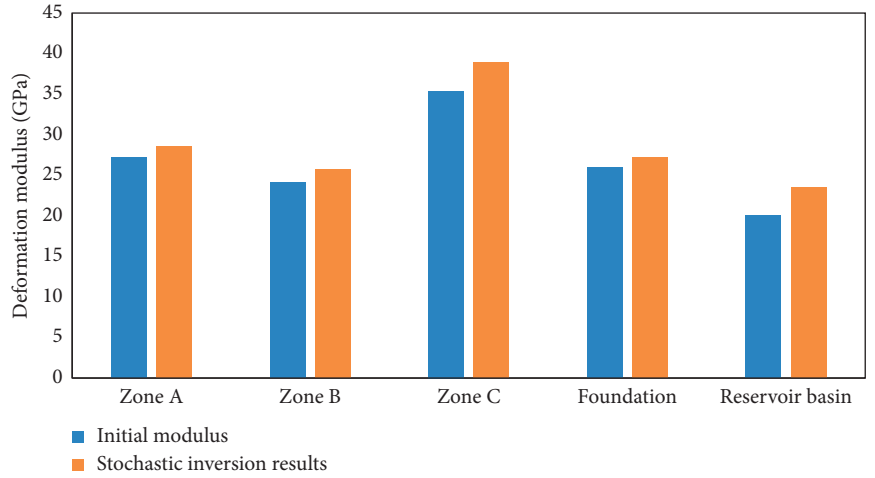

Figure 12: Comparison between the initial modulus and the stochastic inversion results.

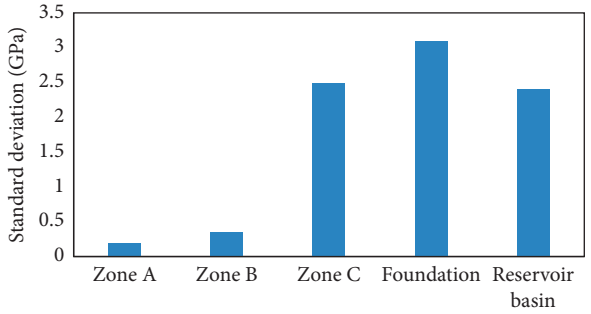

Figure 13: Standard deviation of deformation modulus of different zones.

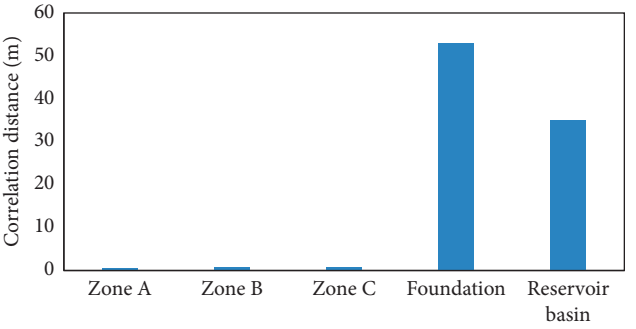

Figure 14: Correlation distance of deformation modulus of different zones.

deviation and correlation distance both appear in the foundation zone. The standard deviation and correlation distance of the reservoir basin are relatively large. And zone C has a much larger standard deviation than the other two dam body zones. This means that the deformation modulus of zone C, foundation, and reservoir basin plays a controlling role in the accuracy of displacement prediction.

6. Conclusions

This study focuses on the stochastic inversion of the elastic and deformation moduli of the dam foundation and the reservoir basin. On the basis of the finite element method, the error function of the stochastic inversion is established using Bayesian back analysis theory, and the implicit and nonlinear relationships between dam displacements and

mechanical parameters are determined using the BP neural network. The FFT algorithm is used to generate the random fields of the undetermined parameters in stochastic sampling, and the Neumann expansion function is used to increase the calculation efficiency of the finite element analysis. Numerical simulation is performed on a certain concrete dam, and the stochastic parameters of the dam body mechanical parameters are obtained by the proposed inverse analysis method. The following conclusions are drawn:

(1) The stochastic inversion method proposed in this paper introduces randomness of mechanical parameters and monitoring data into the inversion procedure which break the limit of conventional inversion method that can only deal with deterministic situation. The mechanical parameters of the dam body, dam foundation, and reservoir basin are viewed as random variables with certain probability distribution and spatial correlation. Thus, the inversion results of the stochastic inversion method put forward can reflect the uncertain characteristics of the mechanical parameters.

(2) The actual zoning deformation modulus of the dam body, foundation, and reservoir basin is put forward based on the comprehensive utilization of SFEM and BP neural network. Furthermore, the objective function of the stochastic inversion is obtained on the basis of Bayesian theory. The results of the inversion case of a certain concrete dam show that the proposed stochastic inversion method is feasible.

(3) The Neumann expansion function is used to increase the calculation efficiency of the stochastic finite element simulation. The FFT algorithm is used to generate random fields efficiently for each sampling of stochastic simulation. The BP neural network has been found to be a fast, accurate, and objective method for nonlinear mapping and increases the efficiency of the optimization by using a small set of training samples.

Notations

A_{lmn}, B_{lmn}: Fourier coefficients
b_j: Output of the hidden layer
C_{e_j}: Stiffness transformation matrix
$\mathbf{E}$, E_i (unit: GPa for deformation modulus): Undetermined mechanical parameters
f: Transfer function
f_i: Probability distribution function
G: One-sided spectral density function
H (unit: m): Hydraulic load
$\mathbf{K}_0$, $\mathbf{K}$, K_{e_j}: Stiffness matrix
$\Delta\mathbf{K}$: Fluctuation value of stiffness matrix
M_k: The kth-order moment
N_s: Sample number
$\mathbf{R}_H$: Node load matrix
$W(d\omega)$: Interval white noise process with zero mean
x_i: Input of the ANN
y_k: Output of the output layer
$Z(x)$: Random field
δ, $\boldsymbol{\delta}$ (unit: mm): Concrete dam deformation
δ_H, $\boldsymbol{\delta}_H$, δ_H^*, $\boldsymbol{\delta}_H^*$ (unit: mm): Hydraulic component
$\boldsymbol{\delta}_H^{\text{cal}}$ (unit: mm): Calculated displacement vector
δ_T (unit: mm): Thermal component
δ_ϑ (unit: mm): Time-effect component
$\boldsymbol{\varepsilon}_{\delta_H^*}$: Measuring error matrix
ζ_j: Threshold value of the hidden layer
ζ_k': Threshold value of the output layer
$\boldsymbol{\eta}_E$: Prior information matrix of $\mathbf{E}$
θ_i, θ_1, θ_2, θ_3, θ_{E_i} (unit: m): Correlation distance
ϑ, ϑ_0 (unit: 1/100 d): Monitoring time
ρ: Correlation of a random variable
$\boldsymbol{\omega}$: Frequency vector
ω_{ij}: Weight from the input layer to the hidden layer
ω_{jk}: Weight from the hidden layer to the output layer
Ω_1, Ω_2, Ω_3: Regions of the dam body.

Data Availability

No additional unpublished data are available.

Conflicts of Interest

The authors declare that they have no conflicts of interest regarding the publication of this paper.

Acknowledgments

This research was supported by the National Natural Science Foundation of China (grant nos. 51739003, 51479054, 51779086, 51579086, 51379068, 51579083, 51579085, and 51609074), National Key R&D Program of China (2016YFC0401601 and 2017YFC0804607), Project Funded by the Priority Academic Program Development of Jiangsu Higher Education Institutions (YS11001), Jiangsu Natural Science Foundation (grant no. BK20160872), Special Project Funded of National Key Laboratory (20145027612 and 20165042112), Key R&D Program of Guangxi (AB17195074), and Central University Basic Research Project (2017B11114).

References

[1] W. Zhongru, G. Chongshi, and S. Zhenzhong, "Theory and application of dam safety synthetical analysis and assessment," *Advances in Science and Technology of Water Resources*, vol. 3, 1998.

[2] G. Yang and M. Yang, "Multistage warning indicators of concrete dam under influences of random factors,"

Mathematical Problems in Engineering, vol. 2016, Article ID 6581204, 12 pages, 2016.

[3] H. Gu, Z. Wu, X. Huang, and J. Song, "Zoning modulus inversion method for concrete dams based on chaos genetic optimization algorithm," *Mathematical Problems in Engineering*, vol. 2015, Article ID 817241, 9 pages, 2015.

[4] J. Song, C. Gu, H. Su, H. Gu, and X. Huang, "Observed displacement data-based identification method of structural damage in concrete dam," *Engineering Failure Analysis*, vol. 66, pp. 202–211, 2016.

[5] G. Yang, C. Gu, T. Bao, Z. Cui, and K. Kan, "Research on early-warning index of the spatial temperature field in concrete dams," *SpringerPlus*, vol. 5, no. 1, p. 1968, 2016.

[6] G. Yang, C. Gu, Y. Zhao, H. Su, Z. Shi, and J. Chen, "Research on an abnormality diagnosis method of the structural behavior of spatial crack systems in concrete dams," *Optik*, vol. 127, no. 24, pp. 11758–11774, 2016.

[7] C. S. Gu and Z. R. Wu, *Safety Monitoring of Dams and Dam Foundations-Theories & Methods and Their Application*, Hohai University Press, Nanjing, China, 2006, in Chinese.

[8] A. De Sortis and P. Paoliani, "Statistical analysis and structural identification in concrete dam monitoring," *Engineering Structures*, vol. 29, no. 1, pp. 110–120, 2007.

[9] A. K. Chopra and J.-T. Wang, "Earthquake response of arch dams to spatially varying ground motion," *Earthquake Engineering & Structural Dynamics*, vol. 39, no. 8, pp. 887–906, 2010.

[10] G. A. Fenton and D. V. Griffiths, *Risk Assessment in Geotechnical Engineering*, Wiley Online Library, Hoboken, NJ, USA, 2008.

[11] S. Rahman and H. Xu, "A univariate dimension-reduction method for multi-dimensional integration in stochastic mechanics," *Probabilistic Engineering Mechanics*, vol. 19, no. 4, pp. 393–408, 2004.

[12] Z. Wu, *Hydraulic Structure Safety Monitoring Theory and its Application*, Higher Education Press, Beijing, China, 2003.

[13] B. Chen, N. Liu, and J. Zhou, "Principle of maximum entropy for back analysis in geotechnical engineering," *Journal of Hohai University*, vol. 30, pp. 52–55, 2002.

[14] J. Yang, D. Hu, and Z. Wu, "Bayesian uncertainty inverse analysis method based on pome," *Journal-Zhejiang University Engineering Science*, vol. 40, no. 5, p. 810, 2006.

[15] X. Cao, C. Gu, and E. Zhao, "Uncertainty instability risk analysis of high concrete arch dam abutments," *Mathematical Problems in Engineering*, vol. 2017, Article ID 6037125, 11 pages, 2017.

[16] J. Zhang and C. Gu, "Maximum entropy method for operational loads feedback using concrete dam displacement," *Entropy*, vol. 17, no. 5, pp. 2958–2972, 2015.

[17] C. Liu, C. Gu, and B. Chen, "Zoned elasticity modulus inversion analysis method of a high arch dam based on unconstrained Lagrange support vector regression (support vector regression arch dam)," *Engineering with Computers*, vol. 33, no. 3, pp. 443–456, 2017.

[18] H.-R. Bae and E. E. Forster, "Improved Neumann expansion method for stochastic finite element analysis," *Journal of Aircraft*, vol. 54, no. 3, pp. 967–979, 2017.

[19] R. G. Ghanem and P. D. Spanos, "Stochastic finite element method: response statistics," in *Stochastic Finite Elements: A Spectral Approach*, pp. 101–119, Springer, New York, NY, USA, 1991.

[20] H. Rue and L. Held, *Gaussian Markov Random Fields: Theory and Applications*, CRC Press, Boca Raton, FL, USA, 2005.

[21] Z. Wu, B. Xu, C. Gu, and Z. Li, "Comprehensive evaluation methods for dam service status," *Science China Technological Sciences*, vol. 55, no. 8, pp. 2300–2312, 2012.

[22] X. P. Liao, H. M. Xie, Y. J. Zhou, and W. Xia, "Adaptive adjustment of plastic injection processes based on neural network," *Journal of Materials Processing Technology*, vol. 187-188, pp. 676–679, 2007.